Further Investigation of Knock Intensity by a Thermodynamic Model and Experiments Using a Rapid Compression Machine

Seiichi Shiga, Gunma University, Kiryu, Gunma 376
Michikata Kono, University of Tokyo, Tokyo 113
Kazuo Iinuma, Hosei University, Koganei, Tokyo 184
Takao Karasawa, Gunma University
Toshio Kurabayashi, Gunma University

ABSTRACT

In a previous work, the substantial meaning of knock intensity in spark ignition engines was made clear by thermodynamic modeling and experiments using a rapid compression machine. In a present study, a finite reaction rate of the spontaneous ignition of an end gas is introduced into the model, while the infinite reaction rate was used in the previous model. This introduction leads to a good agreement between the results of the theory and the experiment. Other disagreements between the model and the experimental results have been also examined. Larger scattering in the values of experimental knock intensity, even when the knock occurred at an equal burned mass fraction by flame propagation, was considered to appear due to a shift of nodal line of the fundamental transverse mode gas vibration in a cylindrical combustion chamber. This supposition is verified experimentally by the present study. Moreover, the mechanism of the gas vibration which occurs when the whole gas mixture in the combustion chamber ignites spontaneously is clarified from the observation by direct and schlieren high-speed photography.

INTRODUCTION

Knock in a spark ignition engine is an essential problem because it gives an upper limit to thermal efficiency and specific output of the engine. Therefore, the phenomenon of knock has long been studied and many informations have been obtained. It is widely accepted that the knock is a sound caused by spontaneous ignition of the end gas which is the last part of the charge to be consumed by the normal flame propagation initiated by a spark plug. Since mass burning rate of the spontaneous ignition is much higher than that of flame propagation, pressure wave is produced and then gas vibration occurs (1). It is generally known that the gas vibration causes some problems such as emission of noise, power loss and thermal troubles due to promoted heat transfer.

From 1930 to 1960, when large spark ignition engines were used as aircraft power sources, a lot of studies to elucidate the knock were carried out. Withrow and Rassweiler(2) took a high-speed direct photograph of the phenomenon and observed a rapid burning of the end gas. Miller(3) and Male(4) took an ultra high speed schlieren photographs of 200000 and 500000 frames per second, respectively, and found the existence of pressure wave when the mixture ignited spontaneously. Ball(5) visually observed rapid propagation of a cool flame which was followed by hot flame generation in a CFR engine. Livengood and Leary(6) found an inhomogeneity of spontaneous ignition in their high speed schlieren photograph by using a rapid compression machine. By an experiment using many ion gaps installed in the combustion chamber of a CFR engine, Curry(7) suggested that the knock might be the result of abnormal acceleration of flame propagation. Affleck(8) concluded that knock is caused by spontaneous ignition of the end gas, by comparing emission of light and combustion products of knocking combustion with those of spontaneous ignition of whole gas mixture using a rapid compression machine.

In spite of the deep understanding of the knock phenomenon, little has been studied about the intensity of knock. In recent years, there has been a growing interest in the problem of knock intensity because of a necessity of knock sensing systems(9) for fuel economy in spark ignition engines. In this area, one of the autors(10) took an oscillating ion current signal detected by an ion gap as a measure of a knock intensity. Hirst and Kirsch(11) made a simulation of a spontaneous ignition process by introducing chemical kinetics. However, in spite of their studies there is little understanding of the relationship between gas vibration and knock intensity. Good(12) and Kumagai and Kimura(13) suggested a thermodynamic consideration and made a correlation of knock intensity with the difference of unbalanced energy level between the portion burned by flame propagation and that by spontaneous ignition.

In a previous report(14), the thermodynamic model based on the consideration by Good(12) and Kumagai and Kimura(13) was made to simulate the combustion processes during flame propagation and spontaneous ignition introducing a chemical equilibrium calculation. At the same time, knock phenomenon was reproduced in a rapid compression machine, where the pressure vibrations were picked up and processed by FFT frequency analysis method. From the experimental approach, some modes of gas vibration were identified and the total vibration energy was obtained by combining an analytical result of wave equation(1) with the measured vibration amplitudes. One of the results is reproduced in Figure 1. As shown in this figure,

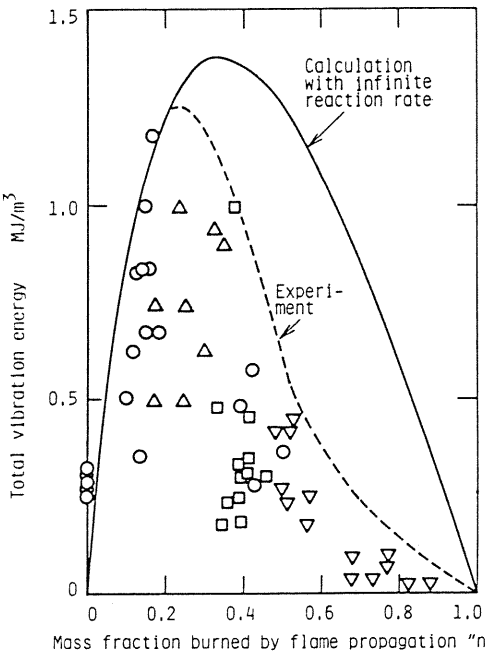

Diethyl ether (mole)	Acetone (mole)	Symbol
1.0	0	○
0.67	0.33	△
0.40	0.60	□
0.18	0.82	▽

Fig. 1 Comparison between experimental knock intensity and calculated one by the previous model (with infinite reaction rate)

the region of the larger value of n.

Two other disagreements are recognized in this figure. One is that the measured knock intensity is not zero at n=0 where a whole gas mixture ignites spontaneously. In the model, of course, no pressure vibration energy is generated under this condition because a homogeneous constant volume combustion is assumed. The experimental fact suggested that the spontaneous ignition could not occur homogeneously. Such inhomogeneity of spontaneous ignition has been observed in some previous studies(6), (15).

The other disagreement between the calculated and the experimental results is large scattering of the experimental value of the knock intensity plotted against the mass fraction burned by flame propagation as seen in Figure 1. This fact suggests the shift of the nodal line of the predominant mode gas vibration.

The purpose of this study is to make clear the causes of the above mentioned disagreements between the calculated and the experimental results. Detailed description of the last two disagreements have already been presented in the other papers (17),(18).

DESCRIPTION OF THE MODIFIED MODEL

Combustion process used in the present model is shown schematically in Figure 2. The fuel-air mixture in the combustion chamber is divided into N elements of equal mass. Each element is labeled by two dimensions, (i,m), where i, numbered from 1 to N, is the order of elements and m represents the time step. The elements from 1 to f are burned by flame propagation and the residual elements from

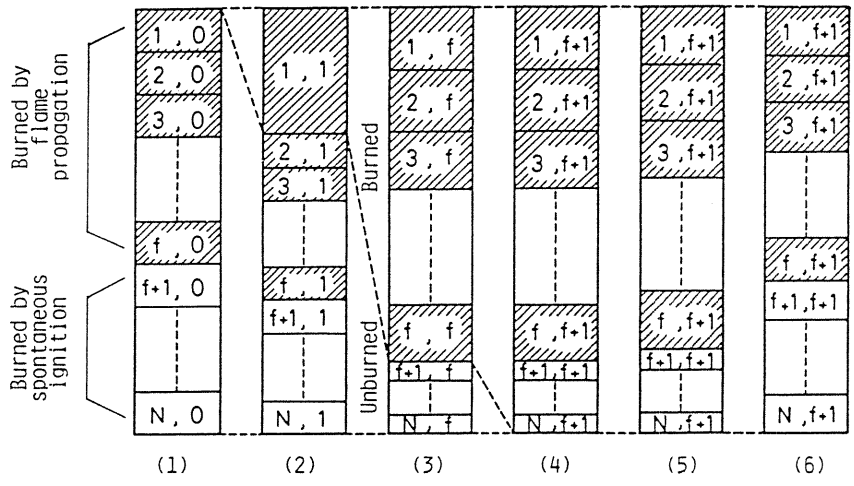

(1) Initial condition
(2) 1st element burned
(3) Flame propagation ends
(4) Spontaneous ignition of end gas with infinite reaction rate
(5) Adiabatic expansion (compression) of end gas (elements burned by flame propagation) due to finite reaction rate
(6) Pressure equilibrated

Fig. 2 Combustion process by gas elements

the qualitative agreement is fairly good and the quantitative one is also good in the region of the smaller mass fractions burned by flame propagation "n". However, the difference between the calculated and the measured values is not small in

(f+1) to N are burned by spontaneous ignition.

At the first step, the step number 0 in Figure 2 (1), flame propagation is going to be initiated by some ignition source, e.g., electric spark, from the first element (1,0). At the next step, step

number 1 in the figure (2), the first element has just been burned by flame propagation. This is simulated by a constant pressure combustion and the subsequent adiabatic compression of all the elements. Flame propagation progresses sequentially to the fth element. At this step, step number f in the figure (3), flame propagation ends. At the (f+1)th step shown in the figure (4), the elements from (f+1) to N are burned by spontaneous ignition which is simulated by a constant volume combustion. This implies an infinite reaction rate. The combustion process from the first step, step number 0 in Figure 2 (1) to the (f+1)th step shown in the figure (4), is the same as used in the previous model. In the previous model, the energy which was assumed to be equivalent to the gas vibration energy, that is knock intensity, was calculated from the step (4) to (6) directly. It is represented by the difference of work between the expansion work of the elements burned by spontaneous ignition and the compression work of the elements burned by flame propagation, as shown in the following relation.

(External work) = (expansion work of(f+1)th---Nth elements) - (Compression work of 1st---fth elements)-------(1)

Both works can be calculated as the difference of the internal energies before and after the adiabatic changes.

In the actual spontaneous ignition process, the reaction rate would not be infinite as shown in Figure 3. It should decrease with increasing ignition delay because reaction rate is inversely proportional to ignition delay. Such dependence of the reaction rate on the ignition delay is also observed in the pressure diagrams in this experiment. When the mass fraction burned by flame propagation is small, which means the ignition delay is shorter, the reaction rate is so large that a large amplitude vibration corresponding to the natural frequency of the pressure transducers is superposed on the pressure diagrams. The natural frequency of the piezo-electric pressure transducers used in this study is 130 kHz. The above fact shows that the pressure transducers can not follow the rapid chemical reaction rate, though they can follow the knock vibration whose frequency is around 10 kHz and is far below the natural frequency of the pressure transducers. When the mass fraction burned by flame propagation is large, such natural vibration of the pressure transducers diminishes and the pressure diagram becomes like the form indicated as "Actual Process" in Figure 3 below. Therefore, it is reasonable to consider that the chemical reaction rate decreases monotonically with increasing ignition delay and accordingly with increasing the mass fraction burned by flame propagation. While the dependence of ignition delay on pressure and temperature has already been presented even in the case accompanying flame propagation (16),(19), it is difficult to take the relationship between the reaction rate and the formation of pressure wave into consideration. Therefore, in this study the dependence of the reaction rate on the mass fraction burned by flame propagation is assumed and it is evaluated that the coincidence between the calculated results and the experimental ones is good or not.

The method for bringing the finiteness of the

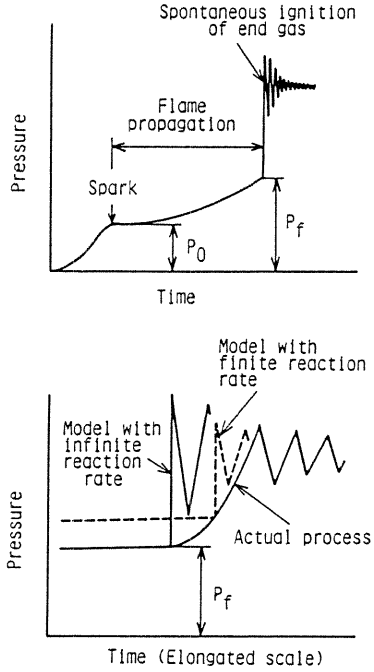

Fig. 3 Schematic pressure records illustrating an actual spontaneous ignition process together with the previous and the present model

reaction rate into consideration is as follows. As described previously, spontaneous ignition occurs at the step (4) in Figure 2. At the next step, a volume change $V_{s,delay}$ due to finite reaction rate is introduced. It is assumed that the elements burned by spontaneous ignition (or flame propagation) expand (or are compressed) adiabatically to the volume to (or from) which $V_{s,delay}$ is added (or subtracted). This is indicated at the step (5) in Figure 2. By adding and subtracting the $V_{s,delay}$, the pressure and temperature of the elements (f+1)---N decrease and those of the elements 1---f increase. From step (5) to (6), the energy equivalent to the knock intensity is calculated by the same manner as previously mentioned. This process is illustrated schematically in Figure 3, where dotted line is the simulated knocking process with taking the finiteness into consideration.

Calculation flow chart is shown in Figure 4. Since the calculation method for flame propagation has been already described in the previous report, only the process after the spontaneous ignition is indicated in this chart. The volume change Vs,delay due to finite reaction rate is expressed in the following relation as indicated in the flow chart.

$$V_{s,delay} = V_0 K n^b \text{ ----------(2)}$$

where V_0 is a volume of the combustion chamber, coefficient K and exponent b are constants which are always positive indicating the monotonic dependence of the reaction rate. The $V_{s,delay}$ is added to the elements burned by spontaneous ignition and subtracted from the elements burned by flame propagation.

$$V'_{s,f+1} = V_{s,f+1} + V_{s,delay} \text{ ----------(3)}$$

$$V'_{b,f+1} = V_{b,f+1} - V_{s,delay} \text{ ----------(4)}$$

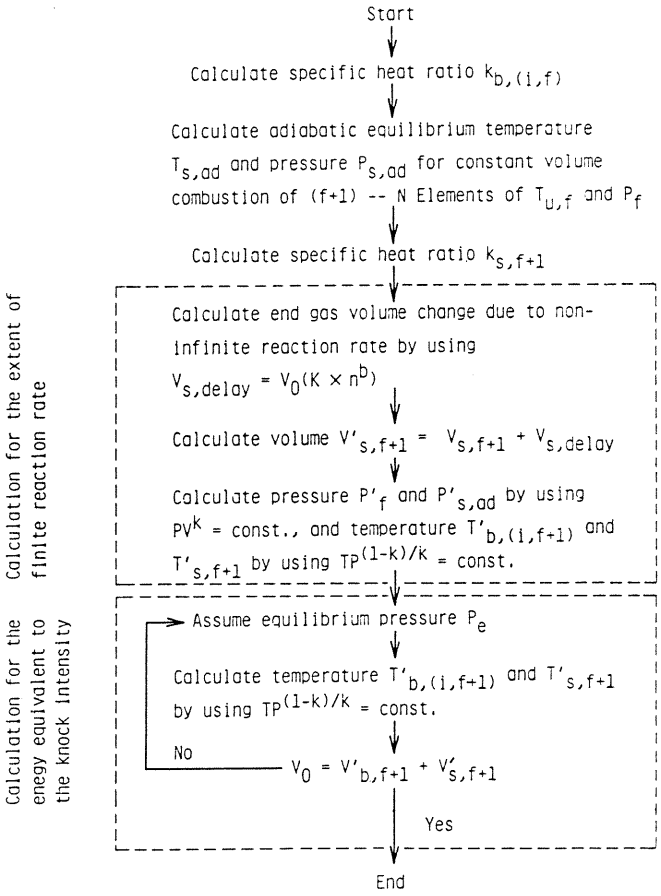

Fig. 4 Flow chart for calculation of spontaneous igniton from (n+1)th to Nth elements with finite reaction rate

where $V_{s,f+1}$, $V_{b,f+1}$ are the volume burned by spontaneous ignition with infinite reaction rate and burned by flame propagation, respectively. The quantities of state such as pressure P'_f, $P'_{s,ad}$ and temperature $T'_{b,(i,f+1)}$, $T'_{s,f+1}$ are then calculated by using the condition of adiabatic change. From this new state $(P'_f, T'_{b,(i,f+1)})$ and $(P'_{s,ad}, T'_{s,f+1})$ to a equilibrated pressure state $(P_e, T'_{b,(i,f+1)})$ and $(P_e, T'_{s,f+1})$, the external work expressed by the equation (1) can be calculated.

RESULTS OF CALCULATION

One of the results calculated by the model described above is shown in Figure 5. Since the model is one-dimensional, the pressure and temperature distributions are expressed against the normalized distance from a spark gap, which is equivalent to a volume fraction burned by flame propagation. The initial condition in this figure is in accordance with that of experiment. Pressure and temperature in (1) are 1.88 MPa and 446 K, respectively, which correspond to the state at the top dead center of the rapid compression machine. The heat loss factor L defined in the previous study is 0.48. The number of segments N is 20. The mixture is stoichiometric diethyl-Ether $(C_4H_{10}O)$ - dry air.

The stage (2) in Figure 5 shows the state at which the 6th element has just been burned by flame propagation, and corresponds to the mass fraction burned by flame propagation n=0.3. Spontaneous

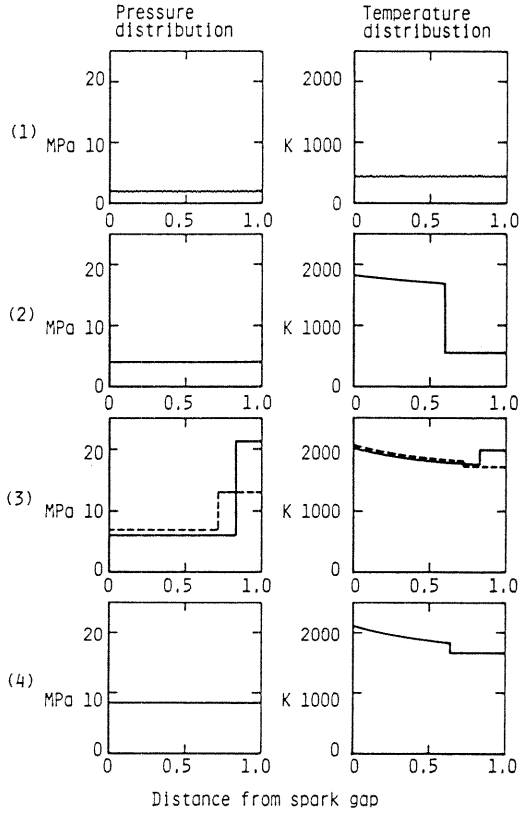

Fig. 5 Pressure and temperature distribution in combustion chamber, stoichiometric (diethyl-ehter)-air mixture. (1); initial conditon corresponding to an experimental condition; (2); mass fraction burned by flame propagation n=0.3; (3); n=0.6 and occurrence of spontaneous ignition. Solid lines indicate the results with infinite reaction rate, dotted lines with finite reaction rate; (4); after pressure equilibration

ignition occurs in stage (3), where n=0.6. Solid lines in both pressure and temperature distributions indicate the state when the end gas (residual mass fraction of 0.4) ignites spontaneously with infinite reaction rate. In the case of finite reaction rate, the end gas expands adiabatically from $V_{s,f+1}$ to $V'_{s,f+1}$ as expressed in equation (3). At the same time, the portion burned by flame propagation is compressed adiabatically. The state just after this change is expressed by dotted lines in stage (3). Spontaneous ignition process of the end gas with finite reaction rate in the present model can be represented by this change from the solid lines to the dotted lines. The volume fraction $V_{s,delay}$ in this case is 0.07 which is obtained from the relation (2). The values of K and b are 0.15 and 1.5, respectively, in this calculation. The external work which is assumed to represent the knock intensity can be calculated from the state indicated by the dotted lines to the pressure equilibrated state (4) in the figure.

The dependence of $V_{s,delay}$ on the mass fraction burned by flame propagation n is not known, but is expected to be monotonic as described previously. Therefore, several combinations of K and b in equation (2) have been examined. As an example, three variations of b at a fixed value of K are expressed in Figure 6. Exponent b is changed from 1 to 2. The results of calculation

are shown in Figure 7. In the case (4) in the figure where Vs,delay is proportional to n, i.e., b=1, the model can not simulate the knock intensity in the region of smaller n, while in the case (2), i.e., b=2, the inclination of the knock intensity seems to be too steep beyond n=0.3. The intermediate value of 1.5 shown as (3) will leads to fit best to the experimental result.

In spite of an introduction of quite simple relation for considering finite reaction rate into the model of spontaneous ignition process, an agreement between the simulated knock intensity and the experimental one is fairly improved. Therefore, it might be concluded that the reaction rate of spontaneous igniton is one of the factors influencing knock intensity.

FURTHER EXAMINATION OF THE PREVIOUS RESULTS

As previously described, there are two other disagreements between the calculation and the experiment. These are examined experimentally.

SHIFT OF NODAL LINE

In a cylindrical combustion chamber, some modes of gas vibration are identified as described in detail in the previous paper. The most prominent mode is the first unsymmetrical transverse one (1,0,0) whose frequency is the lowest. Thus, the experimental data substantially represent this vibration mode which has one diametral nodal line. If this nodal line is formed at a different angle in a different run of the experiment, the amplitude of the gas vibration detected by a fixed pressure transducer will vary even when the mass fraction burned by flame propagation is equal. In order to verify this shift of the nodal line, the following two experiments have been carried out. The first is a simultaneous two-point pressure detection and the second is the use of a rectangular prism combustion chamber in which one-dimensional gas vibration predominates.

The spatial relationship between the spark plug and the locations of the pressure transducers in the first experiment is shown in Figure 8. The experimental results are shown in Figures 9 and 10. Symbols in these figures are indicated in Figure 8. Location A where end gas is formed will be in accordance with the pressure loop position and location B will be the node. The experimental conditions are the same as those shown in Figure 7. In Figures 9 and 10, peak values of damped pressure vibration obtained through a band pass filter whose -3 dB gain points are 7.8 and 11 kHz are shown. In Figure 9, the extrapolated initial peak value of damped pressure vibration detected at location A is about 10 times as large as that detected at location B. In Figure 10, on the other hand, the value at A is only about twice of the value at B. This means that the nodal line in the experiment shown in Figure 9 is much closer to the diameter which is orthogonal to that connecting the location A with the spark plug position than the one shown in Figure 10. From these results, the shift of the nodal line seems to be apparent.

Shape of the combustion chamber in the second experiment is shown in Figure 11 with the cylindrical combustion chamber used in the first experiment. Positions of the spark plug and the pressure transducer are also shown in this figure schematically. In the rectangular prism combustion chamber, one-dimensional gas vibration is predominant and shift of the nodal line will be excluded. The experimental result is shown in Figure 12, where the amplitude of pressure vibration is plotted against the mass fraction burned by flame propagation is shown. Compression

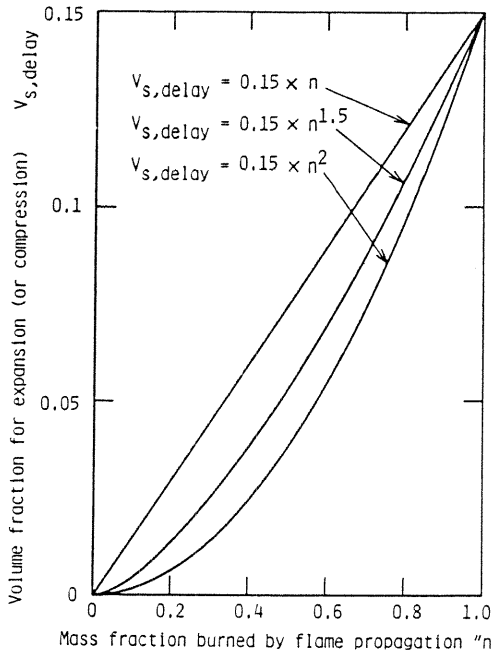

Fig. 6 Variation of assumed volume fraction Vs,delay in equation (2) plotted against at the constant value of K=0.15

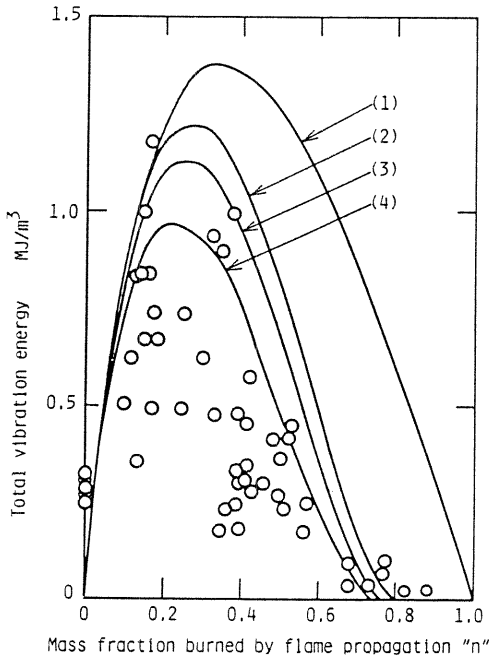

(1) $V_{s,delay}$ = 0 (Infinite reaction rate)
(2) $V_{s,delay} = 0.15 \times n^{2}$
(3) $V_{s,delay} = 0.15 \times n^{1.5}$
(4) $V_{s,delay} = 0.15 \times n$

Fig. 7 Comparison between experimental value of knock intensity and calculated one in which four kinds of reaction rate are assumed as expressed in equation (2)

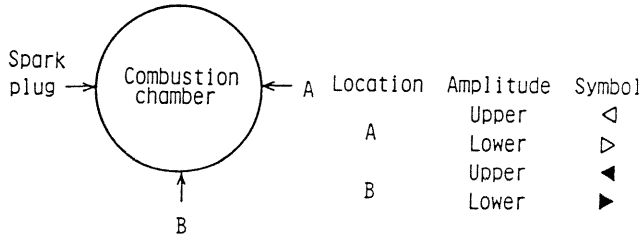

Fig. 8 Arrangement of spark plug and pressure transducers with the symbols used in Figrures 9 and 10.

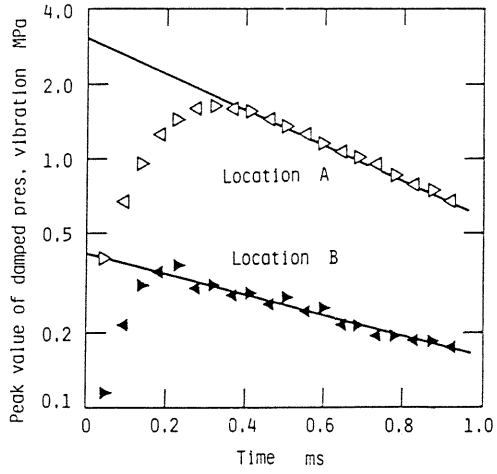

Fig. 9 Variation of peak values of damped pressure vibration with elapsed time, cylindrical combustion chamber

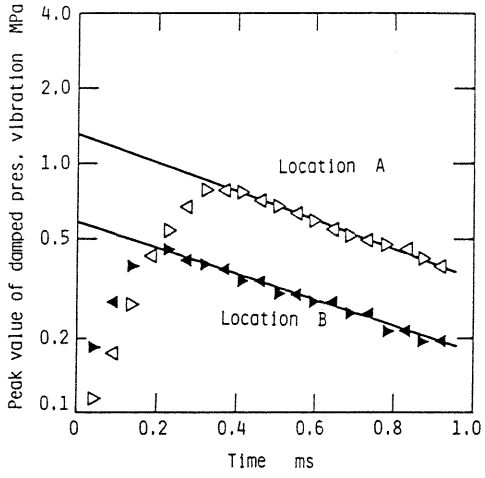

Fig. 10 Variation of peak values of damped pressure vibration with elapsed time, cylindrical combustion chamber

ratio is 10.6 and equivalence ratio of the mixture is 1.0. Scattering of the knock intensity is considerablly decreased comparing with the result in Figure 7. This also shows that the scattering of knock intensity in a cylindrical combustion chamber is mainly based on the shift of nodal line of the pressure vibration.

PHOTOGRAPHIC OBSERVATIONS

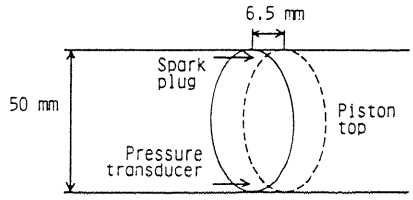

(a) Cylindrical combustion chamber

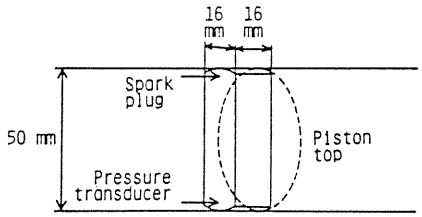

(b) Rectangular prism combustion chamber

Fig. 11 Shape of combustion chamber and positions of spark plug and pressure transducer

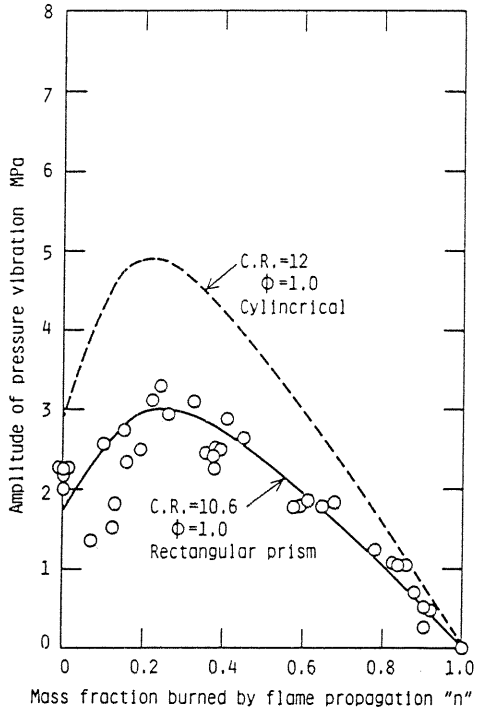

Fig. 12 Variation of knock intensity with mass fraction burned by flame propagation using rectangular prism combustion chamber

As described before, the last disagreement is the generation of gas vibration even when the mass fraction burned by flame propagation is zero as seen in Figures 7 and 12.

Direct photographs are shown in Figures 14 and 17. The former shows a phenomenon accompanying flame propagation and the latter shows that of spontaneous ignition of whole gas mixture. Figures 15 and 16 are the simultaneously detected pressure records corresponding to Figures 14 and 17,

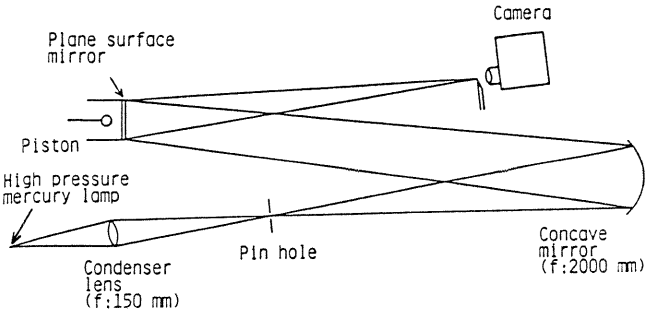

Fig. 13 Schematic diagram of schlieren system

17, it is also observed that hot flame is not generated homogeneously. From these observations of the direct photographs, it is suggested that the first stage of two-stage ignition is not due to a locally generated hot flame and that the hot flame appears inhomogeneously.

High speed schlieren photographs are shown in Figures 18 and 21, and the simultaneously measured pressure records are shown in Figures 19 and 20, respectively. Figures 18 and 19 represent the phenomenon accompanying flame propagation and that of spontaneous ignition of whole gas mixture, respectively. At frames 6,7 and 8 in Figure 18, uniform wrinkled image develops clearly in the end

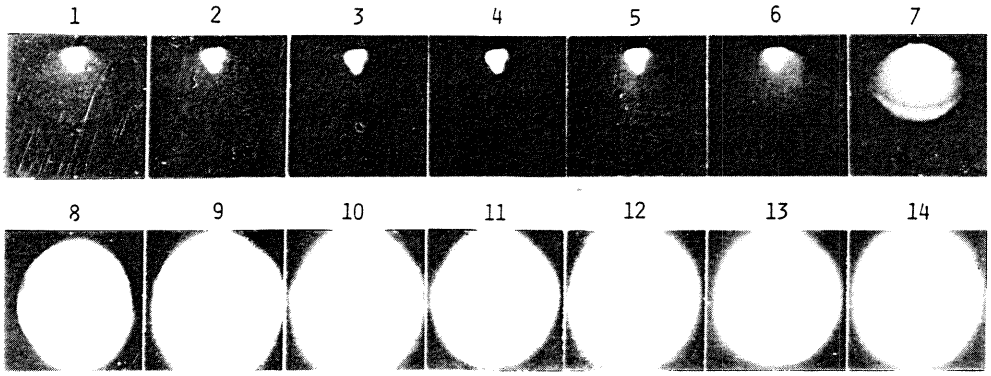

Fig. 14 Direct photograph of knocking combustion, 6000 frames per second, spark plug at upper side, end gas at lower side, spontaneous ignition of end gas occurs at frame 8

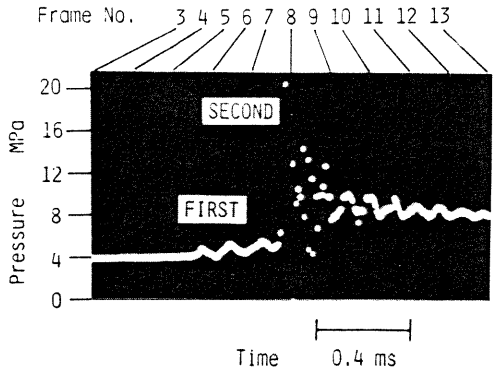

Fig. 15 Simultaneously obtained pressure record, numbers of frames corresponds to that in Figure 14

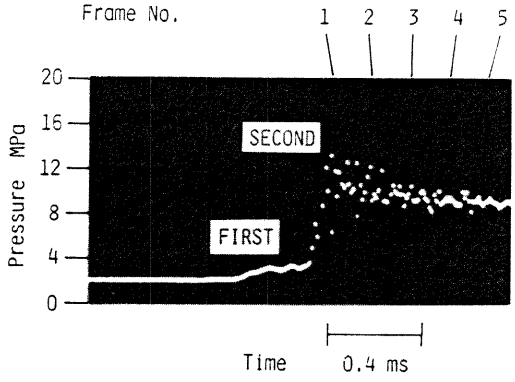

Fig. 16 Simultaneously obtained pressure record, numbers of frames corresponds to that in Figure 17

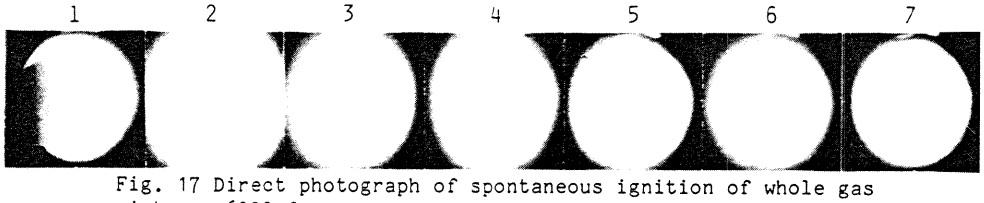

Fig. 17 Direct photograph of spontaneous ignition of whole gas mixture, 6000 frames per second, without spark ignition

respectively. At frames 6 and 7 in Figure 14, no luminescence can be recognized in the end gas region, while a slight pressure rise appears in Figure 15 as designated by "FIRST". When the whole gas mixture ignites spontaneously as shown in Figure 17, any luminescence can not be recognized before the occurrence of an explosive hot flame at frame 1 in spite of the recognition of a slight pressure rise in Figure 16. At frame 1 in Figure gas region. The duration occupied by these frames corresponds to that of the first-stage of two-stage ignition as indicated in Figure 19. Such an image as recognized in the end gas region in Figure 18 also appears at frames 5,6,7 and 8 in Figure 21. The duration occupied by these frames also corresponds to that of the first-stage of two-stage ignition as indicated in Figure 20. These wrinkled images are considered to be a cool flame which has

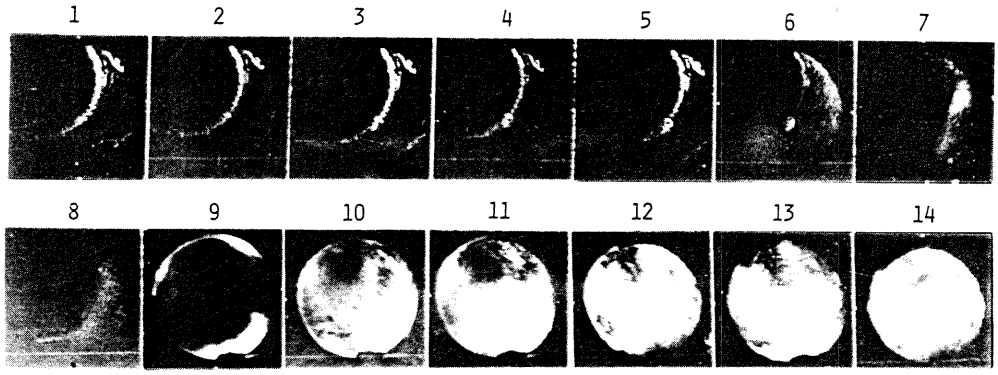

Fig. 18 Schlieren photograph of knocking combustion, 6960 frames per second, spark plug at upper left side, end gas at lower right side, cool flame appears in frames 6,7 and 8 , spontaneous ignition of end gas at frame 9

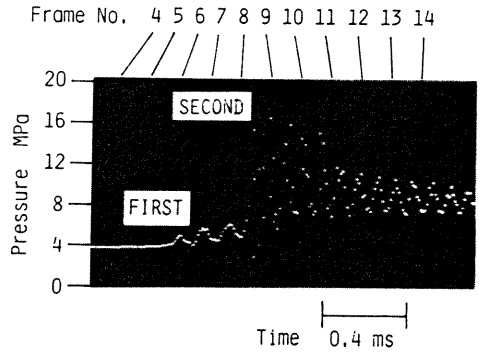

Fig. 19 Simultaneously obtained pressure record, number of frames corresponds to that in Figure 18

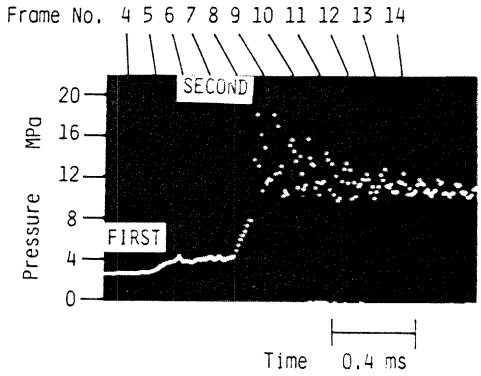

Fig. 20 Simultaneously obtained pressure record, number of frames corresponds to that in Figure 21

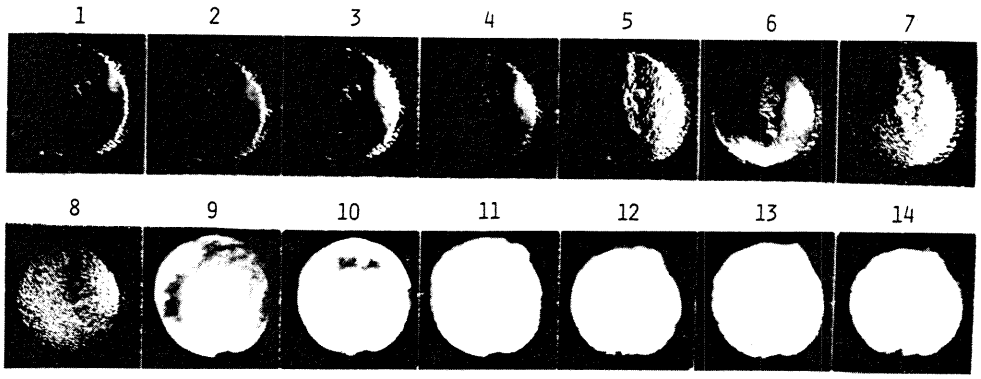

Fig. 21 Schlieren photograph of spontaneous ignition of whole gas mixture, 7620 frames per second, without spark ignition, cool flame appears in frames 5,6,7 and 8, spontaneous ignition at frame 9

not been detected any luminescence in the direct photographs. It is also observed from both Figures 18 and 21 that hot flame appears inhomogeneously.

From the observation of the direct and schlieren photographs, it is seen that the first stage of two-stage igniton is based on a cool flame which gives a wrinkled image to the schlieren photographs and does not give any luminescence to the direct ones, and that the hot flame of spontaneous igniton appears inhomogeneously. This inhomogeneity of hot flame generation is considered to cause a pressure vibration even when the whole gas mixture ignites spontaneously.

CONCLUSIONS

The results of a supplementary study on knock intensity by thermodynamic modeling and experiments using a rapid compression machine are summerized as follows.

[1] The quantitative agreement of the simulated knock intensiy with the measured one is remarkably improved by adopting a modified thermodynamic model. The modification is to take a finite reaction rate into account for spontaneous ignition of the end gas, which was assumed infinite in the previous model. In the actual calculation,

ignition delay which is inversely proportional to reaction rate is introduced.
[2] The diametral nodal line of predominant gas vibration mode in a cylindrical combustion chamber varies its position with every experiment repeated, and causes a scattering of the measured value of knock intensiy.
[3] The fact that gas vibration occurs even when the whole gas mixture ignites spontaneously has been revealed to be based on the inhomogeneous occurrence of hot flame. This hot flame is preceded by the cool flame which gives a wrinkled image to the schlieren photograph, when the spontaneous ignition is accompanied by two-stage igntion.

ACKNOWLEDGEMENT

This work was partly supported by a Grant-in-Aid for Special Project Research from the Ministry of Education, Science and Culture of Japan.

REFERENCES

1. Draper, C.S., "The Physical Effects of Detonation in a Closed Cylindrical Chamber," NACA Rep. No. 493, 1934.

2. Withrow, L. and Rassweiler, G.W., "Slow Motion Shows Knocking and Non-Knocking Explosions," SAE Trans. vol. 39, pp.297, August 1936.

3. Miller, C.D., Olsen, H.L., Logan Jr., W.O. and Osterstrom, G.E., "Analysis of Spark-Ignition Engine Knock as Seen in Photographs taken at 200000 Frames a Second," NACA WTR E-239, May 1946.

4. Male, T., "Photographs at 500000 Frames per Second of Combustion and Detonation in a Reciprocating Engine," Third Symposium (International) on Combustion, Williams & Wilkins Co., Baltimore, pp.721, 1949.

5. Ball, G.A., "Photographic Studies of Cool Flames and Knock in an Engine," Fifth Synposium (International) on Combustion, Reinhold Publishing Corp., New York, pp.366, 1955.

6. Livengood, J.C. and Leary, W.A., "Autoignition by Rapid Compression," Ind. Eng. Chem. vol. 43, pp.2797, 1951.

7. Curry, S., "Effects of Antiknocks on Flame Propagation in a Spark Ignition Engine," Ninth Synposium (International) on Combustion, Academic Press, New York, pp.1056, 1963.

8. Affleck, W.S. and Fish, A., "Knock:Flame Acceleration or Spontaneous Igniton?," Combust. Flame, vol. 12, pp.243, 1968.

9. Kraus, B.J., Godici, P.E. and King, W.H., "Reduction of Octane Requirement by Knock Sensor Spark Retard Syatem," SAE Paper No. 780155, 1978.

10. Iinuma, K., "Studies of Engine Combustion Processes by Ionization Current," Bull. JSME, vol. 4, pp.352, 1961.

11. Hirst, S.L. and Kirsch, L.J., "The Application of a Hydrocarbon Autoignition Model in Simulating Knock and Other Engine Combustion Phenomena," Combustion Modeling in Reciprocating Engine, Plenum Press, New York and London, pp.193, 1980.

12. Good, C.W., "Theoretical Consideration of Power Loss Caused by Combustion Knock," Trans. ASME vol. 64, pp.317, 1942.

13. Kumagai, S. and Kimura, I., "Knock Intensity of Spark Ignition Engine," Science of Machine vol. 5, pp.17, 1953, (in Japanese).

14. Kono, M., Shiga, S., Kumagai, S. and Iinuma, K., "Thermodynamic and Experimental Determinations of Knock Intensity by Using a Spark-Ignited Rapid Compression Machine," Combust. Flame vol. 54, pp.33, 1983.

15. Taylor, C.F., Taylor, E.S., Livengood, J.C., Russel, W.A. and Leary, W.A., "Ignition of Fuels by Rapid Compression," SAE Quart. Trans. vol.4, pp.232, 1950.

16. Lewis, B. and von Elbe, G., Combustion, Flames and Explosions of Gases, Academic Press, New York, Chapter Four, 1961.

17. Shiga, S., Kono, M. and Iinuma, K., "Experimental Study on Knock Intensity of Spark Ignition Engines," JSME Trans. vol. 51, 1985, (in Japanese).

18. Shiga, S., Kono, M. and Iinuma, K., "Study on Knock by High Speed Photographic Observations," JSME Trans. vol. 51, 1985, (in Japanese).

19. Jost, W., "Knock Reaction," Ninth Symposium (International) on Combustion, Academic Press, New York, pp.1013, 1963.